Biochimica et Biophysica Acta, 733 (1983) 201–209
Elsevier

BBA 71809

THE ORIENTATION OF MELITTIN IN LIPID MEMBRANES

A POLARIZED INFRARED SPECTROSCOPY STUDY

HORST VOGEL [a,*], FRITZ JÄHNIG [a], VOLKER HOFFMANN [b] and JÜRGEN STÜMPEL [c]

[a] *Max-Planck-Institut für Biologie, Corrensstrasse 38, D-7400 Tübingen,* [b] *Institut für Physikalische Chemie der Universität Tübingen, Auf der Morgenstelle 8, D-7400 Tübingen and* [c] *Max-Planck-Institut für Biophysikalische Chemie, Am Faßberg, D-3400 Göttingen (F.R.G.)*

(Received March 1st, 1983)

Key words: Membrane-protein interaction; Melittin orientation; Infrared spectroscopy; Linear dichroism; (Phospholipid membrane)

Polarized infrared spectra of melittin incorporated into macroscopically oriented lipid membranes are reported. From the linear dichroism of the amide I and amide II vibrational bands, the spatial orientation of the melittin helices was determined as being preferentially parallel to the membrane normal, under our experimental condition of low water content and an ordered lipid phase. Considering the various models for the orientation of melittin in lipid membranes proposed in the literature, we conclude that our data are in accord with an arrangement whereby the hydrophobic part of the polypeptide either spans the bilayer in the form of two bent helix segments, or is folded back within one monolayer in the form of a wedge.

Introduction

The amphiphatic polypeptide, melittin, has been widely used as a simple model compound for the study of the interaction of proteins with lipid membranes (for a short review see Ref. 1). The effect of melittin on lipid order has been established by using different experimental techniques [2–5]. To date, however, the spatial arrangement of melittin within the lipid bilayer has not been unambiguously determined.

The sequence of melittin contains a largely hydrophobic segment of amino acids 1–20 and a hydrophilic region of amino acids 21–26, carrying four positive charges (H_2N-Gly-Ile-Gly-Ala-Val-Leu-Lys-Val-Leu-Thr-Thr-Gly-Leu-Pro-Ala-Leu-Ile-Ser-Trp-Ile-Lys-Arg-Lys-Arg-Gln-Gln-NH_2). Using the hydrophobicity index (HI) of Segrest and Feldmann [2] with an assumed HI = −2 for the lysine-7, we calculate a value of HI = 2.2 for the hydrophobic segment 1–20 of melittin. This is fairly high, and comparable to the intramembraneous domains of typical membrane proteins such as glycophorin (HI = 2.8, residue 37–59), the fd phage coat protein (HI = 2.6, residue 27–39) and cytochrome b_5 (HI = 2.0, residue 91–130).

In dilute aqueous solution melittin adopts a monomeric highly flexible extended chain with 7% α-helix content, whereas the membrane bound polypeptide consists of 70% α-helical regions as determined by circular dichroism measurements. The average conformation is the same, independent of whether different lipid membranes or micelles are used [7,8]. A similar conformational change is observed due to self-association in aqueous solution if the polypeptide concentration or ionic strength is increased [8–10]. It therefore ap-

---

[*] To whom correspondence should be addressed.

Abbreviations: DMPC, 1,2-dimyristoyl-*sn*-glycero-3-phosphocholine; DTPC, 1,2-ditetradecyl-*sn*-glycero-3-phosphocholine.

pears that the α-helical form of melittin results from a hydrophobic environment, which may be the hydrocarbon phase of the lipid membrane or the hydrophobic side-chains of neighboring peptides in the self-aggregated form.

Recently, the molecular structure of crystalline melittin has been reported at a resolution of 2 Å [11]. The molecules are arranged in tetramers. Residues 1–10 and 13–26 form two α-helices, with an angle of 120° between the helix axes, giving the molecule the form of a bent rod. The helix content of this structure (90%) is higher than in the lipid membrane (70%), because the hydrophilic segment 21–26 adopts different conformations in the crystal and in the lipid bilayer. From very recent NMR experiments a structure of detergent bound melittin was deduced, where at least the 16–20 residue segment adopts a helix-like conformation and the hydrophilic 21–26 residue part is located in the water phase without defined conformation [12]. Since in the case of lipid bilayers the hydrophilic part is also located in the water phase, it again should adopt a disordered conformation, leading to the α-helix content of 70% which is attributed to residue 1–20.

The three-dimensional structure of melittin was calculated from its amino acid sequence by two different groups. In a first report [13] the Chou-Fasman analysis was applied, resulting in a conformation with two helical segments 2–11 and 15–20, which is 65% of the peptide, a hinge region 12–14 and a random part 21–26. In a second publication [14], only the structure of the 1–20 segment of melittin was evaluated, and two very similar low-energy conformations with a helical content of 73–65% for the 26 amino acid residue peptide were found. In one structure the regions 1–12 and 14–20 are α-helical, in the other structure the α-helices range from 1–10 and 14–20. Again a bent region was present before proline-14. Thus, the structure of the hydrophobic segment 1–20 derived theoretically and that determined from X-ray diffraction are in good agreement. As there is the same α-helix content of segment 1–20 in the crystal, in the tetramer in aqueous solution, in micelles and in lipid bilayers, it is reasonable to postulate a common bent rod conformation for all these cases. This is supported by the fact that the ^{1}H-NMR spectrum of tetrameric melittin in aqueous solution is largely identical with the spectra of melittin bound to various detergent micelles [15] (see Table I for a summary of the structural data on melittin).

Given the conformation of melittin in the bilayer, the question of its spatial arrangement is a matter of the orientation of the bent rod in the bilayer. This could range from a situation where the helical segments of the molecule are oriented preferentially in the membrane plane to the case where they are oriented perpendicular to this plane. In the present work, we have undertaken polarized infrared spectroscopy of melittin bound to macroscopically oriented multilamellar membranes in order to determine the orientation of the α-helical segments in the lipid bilayer.

This method has previously been applied to study the orientation of α-helix segments of bacteriorhodopsin in purple membranes [16], of rhodopsin in photoreceptor membranes [17], of intrinsic proteins in photosynthetic membranes [18] and of gramicidin A incorporated into DMPC membranes [19].

Materials and Methods

Sample preparation

DTPC was synthesized according to the method described in Ref. 20. DMPC was purchased from Fluka. Thin-layer chromatography in different solvent systems showed that the samples were homogeneous. Phospholipase-free melittin was prepared as described previously [7]. Regarding the interaction with melittin, DTPC shows behavior similar to that of DMPC. Melittin binds strongly to an aqueous dispersion of DTPC membranes; at a molar ratio DTPC/melittin greater than 50, the mean conformation of the polypeptide is about 70% helix as in the case of DMPC (Vogel, H., unpublished data).

Lipid-melittin membranes for the infrared experiments were prepared in the following way. Distilled water was added to the dry lipid powder to give a $2 \cdot 10^{-2}$ M lipid dispersion which was stored for 1 h at 35°C, i.e., at a temperature above the ordered ↔ fluid phase transition, followed by a 1 min vortex mixing. Equal volumes of melittin solutions in water and lipid dispersions were mixed to give a molar lipid/melittin ratio of 70 in the case of DTPC and of 100 in the case of DMPC. After storing the lipid-melittin mixtures for 1 h at 35°C, the samples were centrifuged at room temperature for 1 h at $300000 \times g$. The supernatant was discarded, in order to remove non-membrane-associated melittin. The pellets were resuspended in water to give a lipid concentration of $2 \cdot 10^{-2}$ M. 100–500 μl of a membrane suspension was loaded to an Irtran-4 plate and dried in a vacuum desiccator over silica-gel at room temperature.

This method resulted in a preferential orientation of the membrane fragments in the plane of the plate. After drying, the samples were equilibrated for 2 h over a saturated aqueous solution of LiCl at 60°C, giving lipid membranes of about 6% (w/w) water content, which corresponds to 2–3 water molecules per lipid molecule. Under these conditions, the membranes of DTPC and DMPC are in the ordered state at room temperature. For a specific density of the membranes of about 1 g/ml, the thickness of the ordered multilamellar membrane films was calculated to range from 3 to 13 μm.

Spectroscopic measurements

Infrared absorption spectra were obtained with a Perkin-Elmer 180 double-beam spectrometer, equipped with polarizers in the sample and in the reference beam. Polarization was either parallel or perpendicular to the plane defined by the direction of the incoming beam and the membrane normal (Fig. 1A). In the case of DTPC-melittin membranes, the angle of incidence of light, α_0, was varied between 0 and 60° in steps of 15°; for DMPC-melittin membranes, only $\alpha_0 = 0°$ and 60° was employed. A blank Irtran-4 plate of identical geometry was placed in the reference beam. To correct for lipid and water absorption, spectra of the corresponding lipid films without melittin were recorded. As a further control, the membrane film was washed off from an Irtran-4 plate with methanol and the washed plate measured in the sample beam. No difference was observed compared to a blank plate, indicating that no lipid or melittin was irreversibly dissolved in the Irtran-4 plate in a non-bilayer form. The spectral resolution was 2–4 cm^{-1}, all measurements were made at room temperature.

Analysis of infrared measurements

From the absorption spectrum of a lipid-melittin membrane, the absorption spectrum of the corresponding pure lipid membrane is subtracted using the lipid bands at 1468 and 1378 cm^{-1} as internal standards. The resulting spectrum of pure melittin contains non-dichroic components which arise mainly from the random-coil segments of membrane-bound melittin (Table I). These can be eliminated from the experimental intensities for parallel ($A^{\parallel}$) and perpendicular ($A^{\perp}$) polarization in the following way [18] to yield the components of the helical segments alone:

$$A_h^{\parallel} = A^{\parallel} - (1 - f_h)(A^{\parallel} + 2A^{\perp})/3$$

$$A_h^{\perp} = A^{\perp} - (1 - f_h)(A^{\parallel} + 2A^{\perp})/3$$

with f_h denoting the fraction of helical content. Here the assumption was made that the helical and random coil components have identical extinction coefficients, as was observed for polylysine [21]. From the final intensities of the amide I (1657–1658 cm^{-1}) and amide II (1542 cm^{-1}) bands, the dichroic ratio follows as $R = A_h^{\parallel}/A_h^{\perp}$. Band heights were used for evaluation, but use of band areas gave the same results within experimental error.

From the dichroic ratio R, the orientational order parameter, S, of the amide transition dipoles is derived via the relation

$$R = 1 + \frac{3S}{1 - S}\sin^2\alpha \tag{1}$$

The angle, α, between the direction of the incoming light in the membrane and the membrane normal is calculated from Snell's law, $\sin\alpha_0 = n \sin\alpha$, with the refractive index of the membrane $n = 1.55$ [22]. This order parameter can further be expressed as the product of three order parameters

$$S = S_t S_h S_m \tag{2}$$

S_t refers to the orientation of the transition moment with respect to the α-helix axis, S_h describes the average orientation of the α-helix axis with respect to the membrane normal, and S_m takes account for the mosaic spread of the sample. (For a detailed discussion see Ref. 16.) Eqn. 2 holds

TABLE I

SUMMARY OF STRUCTURAL DATA OF MELITTIN FROM THE LITERATURE

The percentages or the residue numbers of the corresponding conformational regions are presented.

System	Method	α-Helix region	Bent region	Random region	Ref.
Melittin/lipid membranes	CD	70%		30%	7,8
Melittin/detergent					
Melittin tetramer, aq. soln.	CD	70%		30%	8,9,10
Melittin/detergent [a]	^{1}H-NMR	16–20		20–24	12
Melittin tetramer, crystal	X-ray	1–10 13–26	11–12		11
Melittin, hydrophobic environment	calculation from sequence	2–11 15–21	12–14	22–26	13
	[b]	1–12 14–20	13		14
	[b]	1–10 14–20	11–13		14

[a] Only the structure of the segment 16–24 was investigated.

[b] Only the structure of the segment 1–20 was calculated.

when the helices are symmetrically distributed around the membrane normal, leading to a uniaxial symmetry of the oriented membrane stack. For ideally oriented multilamellar membrane stacks $S_m = 1$. The mosaic spread of air-dried oriented lipid membranes has been measured recently by neutron scattering to be approx. 15° [23]. Because our samples are prepared in a similar way, we assume $S_m = 0.9$. For the amide I vibration, $S_t = 0.41$ and for the amide II vibration, $S_t = -0.40$ [16,18]. With known S_m and S_t, the average orientational order, S_h, for melittin can be determined from the measured order parameter S. Two independent values of S_h are obtained from amide I and amide II bands. The orientational order parameter S_h is correlated to the average orientation according to

$$S_h = \langle \frac{3\cos^2\theta - 1}{2} \rangle \tag{3}$$

θ is the angle between the preferred axis, the bilayer normal, and the helix axis. The angular brackets denote the average over the distribution of helices in the membrane.

Results

Based on CD measurements, we have recently shown that only a limited amount of melittin can be bound to lipid membranes [7]. In the case of DMPC, about 50–100 lipid molecules are necessary to bind one melittin molecule. All our experiments were therefore performed at low concentration of melittin within the membrane in order to be sure that all molecules of the polypeptide are bound to the membrane. Unfortunately, the use of membranes of diacylphospholipids with low melittin concentration causes difficulties in determining the exact linear dichroism of the amide I vibrational band, because the very strong lipid C=O stretching band at 1738 cm^{-1} overlaps the weak peptide vibrational band around 1658 cm^{-1}. Our strategy was therefore first to use lipid membranes of DTPC, where the lipid hydrocarbon chains are linked via an ether bond to the glycerol backbone of the polar group. DTPC shows no strong vibrational bands in the spectral range of the amide I region. In a second experiment, melittin was bound to oriented membranes of DMPC to investigate whether the differences in the glycerol region of

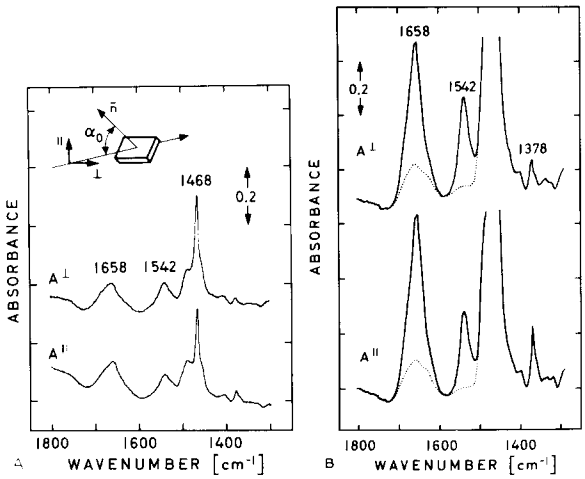

Fig. 1. Polarized infrared spectra of oriented multilamellar membranes with a molar ratio DTPC/melittin of at least 70 at room temperature. (A) The angle between incoming light and the membrane normal, $\vec{n}$, was $\alpha_0 = 60°$. The polarization was parallel ($A^{\parallel}$) or perpendicular ($A^{\perp}$) to the plane between incoming beam and membrane normal, as indicated by the scheme at the top. The strong band at 1468 cm^{-1} results from CH_2-bending vibrations of the lipid hydrocarbon chains. The units of the absorbance axes are 0.2 absorbance units . (B) Conditions as in (A) but with a 5-fold higher film thickness. The dotted lines correspond to spectra of a DTPC membrane film prepared and measured under conditions identical to those of the DTPC-melittin sample. The spectra of the DTPC membrane film were multiplied by a factor such that the intensities, $A^{\parallel}$ and $A^{\perp}$, of the 1378 cm^{-1} CH_3 bending mode of the lipid chains coincide with those of the DTPC-melittin sample.

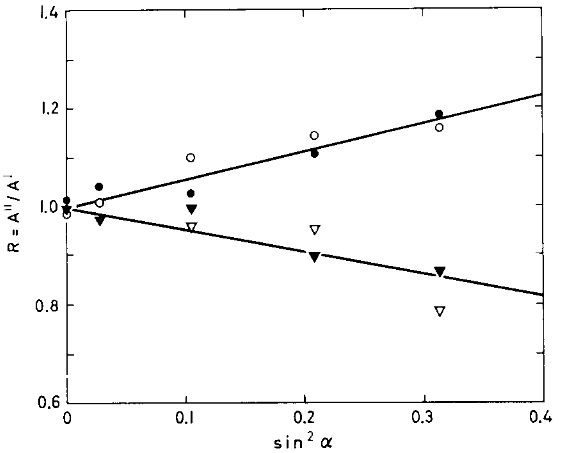

Fig. 2. The dichroic ratio, $R = A^{\parallel}/A^{\perp}$, of the amide I (circles) and amide II (triangles) vibrational bands of melittin in DTPC membranes (molar ratio DTPC/melittin ⩾ 70) as a function of $\sin^2\alpha$. Data of two different samples are shown.

the lipids influence the orientational order of the peptide chain.

Fig. 1 shows infrared spectra of DTPC-melittin membranes in the range between 1800 cm^{-1} and 1400 cm^{-1} with parallel and perpendicular polarized light at $\alpha_0 = 60°$. Two samples with different film thickness were prepared in order to demonstrate the effect of melittin on the lipid bands and furthermore to show the amide bands with a sufficiently high intensity. The band at 1468 cm^{-1} arises from a CH_2 bending mode of the lipid hydrocarbon chains and shows a dichroic ratio of $R = 0.79 \pm 0.02$ with and without melittin (Fig. 1A). These data are in good agreement with those published for other lipid films, and correspond to a tilt angle of 22°C between the lipid chains and the disk normal (Ref. 19, and references therein). Since the tilt angle between the lipid chains and the membrane normal is expected to be 15° for phosphatidylcholines at the given water content [24], we conclude that the lipid chains are correctly

TABLE II

EVALUATION OF THE AVERAGE ORIENTATION OF MELITTIN α-HELICES FROM LINEAR DICHROISM

		Amide I		Amide II	
		$f_h = 1$ $S_m = 1$	$f_h = 0.7$ $S_m = 0.9$	$f_h = 1$ $S_m = 1$	$f_h = 0.7$ $S_m = 0.9$
DTPC/melittin ⩾ 70	S_h	0.39	0.59	0.48	0.78
	θ	40°	32°	36°	23°
DMPC/melittin ⩾ 100	R ($\alpha_0 = 60°$)	1.3 ± 0.1		0.86 ± 0.04	
	S_h	0.60	0.87	0.44	0.73
	θ	31°	17°	38°	25°

oriented within the membranes and the membranes are oriented parallel to the disk plane. Because no effect of melittin on the dichroism of the lipid bands was observed, the use of a pure lipid spectrum as the baseline in a lipid-melittin spectrum is justified.

The wavenumbers of the amide I (1658 cm^{-1}) and amide II (1542 cm^{-1}) bands indicate a mainly α-helical melittin conformation [25], in agreement with the CD data [7]. The resulting dichroic ratios, R, of the amide I and amide II bands measured at various angles α_0 show a linear dependence on $\sin^2\theta$ (Fig. 2), as expected from Eqn. 1. From the slope of the curves the order parameter, S, is determined. Without any correction, i.e., under the assumption of a 100% helical polypeptide ($f_h = 1$) and a perfect membrane orientation ($S_m = 1$) we obtain from Eqn. 2 a lower limit for the orientational order parameter: $S_h = 0.39$ from amide I and $S_h = 0.48$ from amide II. A more realistic value for S_h is obtained by taking into account that 70% of the melittin conformation is helical, whereas 30% is random (Table I), and that the mosaic spread leads to a value of $S_m = 0.9$ (see Materials and Methods). We then calculate $S_h =$ 0.59 for amide I and $S_h = 0.78$ for amide II (Table II).

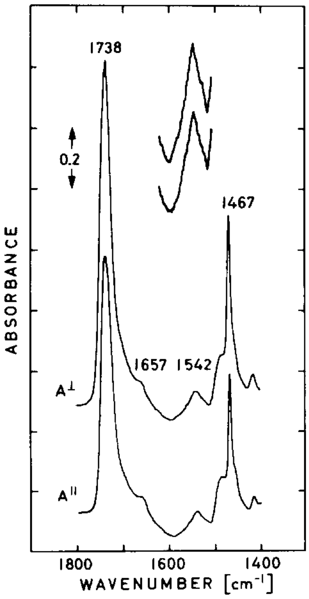

Fig. 3. Polarized infrared spectra of oriented multilamellar membranes of DMPC/melittin ⩾ 100 at room temperature. The amide I bands are shown expanded in the upper part of the figure.

In the case of DMPC-melittin membranes at $\alpha_0 = 60°$ the linear dichroism of the CH_2 bending mode at 1467 cm^{-1} of the lipid chains yields $R = 0.79 \pm 0.02$ and that of the C=O stretching mode at 1738 cm^{-1} of the lipid carboxyl groups $R = 0.78 \pm 0.02$. These values again demonstrate that the lipid chains are well oriented [19]. As in the case of DTPC, no difference was observed in the dichroism of the lipid bands in DMPC membranes with and without melittin. The linear dichroism of the amide I and amide II bands (Fig. 3) leads to values of $S_h = 0.60$ and 0.44 as a lower limit and to $S_h = 0.87$ and 0.73, respectively, applying the described corrections (Table II). Here the dichroism of the amide I band cannot be as accurately determined as that of the amide II band because of the very intense 1738 cm^{-1} band of the lipid carboxyl group. Nevertheless, the evaluation of R for the two amino bands leads to similar S_h values. The nearly identical S_h deduced from the amide II dichroism in DTPC and DMPC membranes implies that there is no difference in the mean orientation of the melittin helices in the two membranes.

Our results are at variance with a former study of the interaction of melittin with egg-phosphatidylcholine and phosphatidylethanolamine multilayers [26], where no dichroism of the amide I and amide II bands was observed with oriented membrane preparations. We believe that these findings are due to the authors' use of a very high concentration of melittin, giving preparations where a considerable part of the polypeptide was not bound to the lipid membranes. From a comparison of the intensities of the amide II mode and the lipid CH_2 bending mode, we estimate a total molar lipid/melittin ratio of 10–20 (Figs. 1B and 2E in Ref. 26). According to the described sample preparation – first the lipid film was deposited on an AgCl plate which was then soaked with an aqueous solution of melittin – it is not certain that all lipid bilayers are equally well accessible to melittin during this procedure. The local lipid/melittin ratio therefore may be even lower than 10–20. This implies that not all melittin molecules are incorporated in the lipid membranes, since 50–100 lipid molecules were found to be necessary for binding one molecule of melittin [7].

Discussion

The conclusion drawn from our results is that the α-helices of membrane-bound melittin are predominantly oriented perpendicular to the membrane plane, as can be seen from the order parameter $S_h = 0.69$ in DTPC (average of the order parameter determined from amide bands) and $S_h = 0.73$ in DMPC membranes (from amide II band). For a further interpretation of S_h we proceed in a manner analogous to the treatment of the order parameter of the lipid chains in membranes. The orientational order parameter, as determined by, for example, NMR measurements, was characterized as a product of two order parameters, one describing the rigid-body order and the other the conformational order of the lipid chains [27,28]. In the case of a helical polypeptide in a lipid membrane this leads to

$$S_h = S_h^{\text{rigid}} \cdot S_h^{\text{conf}} \qquad (4)$$

where S_h^{rigid} and S_h^{conf} define the rigid-body and the conformational order of a helix, respectively.

S_h^{conf} is influenced by the static molecular conformation and the intramolecular flexibility. Not much is known about the internal flexibility of membrane proteins at present. Recent NMR measurements with specifically deuterated bacteriorhodopsin in the purple membrane demonstrate that the β-CD_2 groups of the amino acid side-chains are immobilized as in a crystal, implying the absence of internal flexibility and rigid-body motion of the helical segments [29]. A bigger effect on S_h^{conf} in the case of melittin may arise from conformational flexibility within the hinge region. As mentioned already, Pincus et al. [14] have calculated that two stable conformations of comparable energy exist, differing in the hinge region.

If we assume that the conformation of melittin is a bent rod oriented along the membrane normal with the same angle, θ, between the two helix segments and the membrane normal, and excluding any flexibility or rigid-body motion, we obtain

$$S_h = S_h^{\text{conf}} = \frac{3\cos^2\theta - 1}{2} \qquad (5)$$

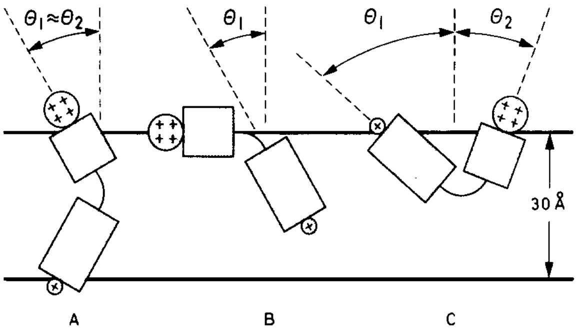

Fig. 4. Models for the spatial arrangement of a melittin molecule in a lipid bilayer, the hydrocarbon part of which is assumed to be 30 Å. Melittin is composed of two helices, represented by the two rectangles with a diameter of 10 Å and a rise of 1.5 Å per residue. Helix 1 (residues 1–11) and helix 2 (residues 14–20) are connected by a bent region (residues 12–13). θ_1 and θ_2 are the angles between the axis of helix 1 and helix 2 and the membrane normal. One positive charge at the N-terminus and the four positive charges in the hydrophilic part (amino acid 21–26) of the molecule are shown, but the positive charge of Lys-7 is omitted, because this side-group may be decharged when inserted into the membrane. (A) Melittin traverses the hydrophobic part of the bilayer, $\theta_1 \approx \theta_2$, with an angle, θ_b, of approx. 120° between the helix axes. The orientation of the average helix axis is the membrane normal. (B) A model proposed by Terwilliger et al. [11]. Helix 1 is directed to the hydrophobic lipid region with $\theta_1 = 30°$, whereas helix 2 lies in the membrane plane with $\theta_2 = 90°$ and $\theta_b = 120°$. (C) Melittin dips only into one half of the bilayer. The average helix axis is oriented preferentially parallel to the membrane normal with $\theta_1 = \theta_2 = 20$–$30°$ and $\theta_b = 40$–$60°$.

From θ, the angle, θ_b, between the two helix axes is calculated as $\theta_b = \pi - 2\theta$. The measured values of S_h yield $\theta = 27°$ for DTPC and $\theta = 21°$ for DMPC, or $\theta_b = 126°$ and 138°, respectively. These values for θ_b are in good agreement with the crystallographic result of $\theta_b \approx 120°$. Thus, the model of a bent rod oriented along the membrane normal, as shown in Fig. 4A, is compatible with our experimental results. In this model, the conformation of melittin is the same as that derived from X-ray diffraction [11] and theoretical calculations [14]. As pointed out in Ref. 11 the bent-rod conformation is consistent with the molecule spanning the hydrophobic part of the membrane (about 30 Å). Within this model, the observed order parameter, S_h, does not permit intramolecular flexibility nor rigid-body motion. Internal flexibility and rigid-body motion would indeed be expected to be small for a peptide in the ordered phase of a lipid bilayer, as in our case.

Our experimental result excludes several other models proposed for the orientation of melittin in the membrane, although various arrangements are still possible. Terwilliger et al. [11] favored the hypotehsis that melittin binds to membranes with its helix axes lying mainly parallel to the bilayer plane (Fig. 4B). The measured order parameter, S_h, is an average value between the order parameter of the eleven-residue N-terminal helix S_{h1} and the seven-residue C-terminal helix S_{h2} with $S_h = (11S_{h1} + 7S_{h2})/18$. Using this relation and Eqn. 5 with $\theta_1 = 30°$ and $\theta_2 = 90°$ from the model B, we obtain $S_h = 0.19$, in total disagreement with our experimental finding.

Terwilliger et al. [11] supposed an insertion of the polypeptide as in Fig. 4A to be unlikely, because in this case the relatively hydrophilic amino acids Lys-7, Thr-10, Thr-11, Ser-18 would be placed in the hydrophobic membrane portion. On the other hand, when the helices are inserted as in Fig. 4B, all the hydrophilic side-chains, which are segregated to one side of the bent rod, can be located at the lipid/water interface. Several arguments can be put forward, however, in favor of model A. First, within the α-helical segment, the polar side-chain of Lys-7 could easily form a hydrogen bond to the hydroxylic group of Thr-11, thereby partly reducing the energetic cost for inserting this side chain into the hydrophobic lipid region. Engelman and Seitz [30] have estimated the transfer free energy of a lysine side-chain from an aqueous to a non-polar environment to be approx. 10 kcal/mol. This value will be reduced to approx. 5 kcal/mol by the formation of hydrogen bonds in the α-helix. Furthermore, the OH-groups of Thr-10 and Ser-18 may be involved in hydrogen bonds to Leu-6 and Pro-14, respectively [14].

Second, there exists the possibility that several melittin molecules aggregate within the membrane in such a way that the hydrophilic sides of the mainly hydrophobic α-helical segments face one another. Preliminary fluorescence energy transfer studies between suitably labeled melittin molecules indicate that oligomers of the peptide are present in the membrane both below and above T_t (Vogel, H., unpublished data). Overall, the energy gained from incorporating the whole of the hydrophobic helical regions of melittin into the apolar membrane milieu more than compensates for the few kcal/mol necessary for insertion of the polar residues into the membrane [31].

Another model is that of a wedge as shown in Fig. 4C. An extreme form of this model with $\theta_1 = 90°$ and $\theta_2 = 30°$ was proposed by Dawson et al. [13], but this leads to $S_h = 0$ and thus is again in contradiction to our experimental findings. Schoch and Sargent [32] have interpreted their experimental results as evidence for this model. Using black lipid membranes of egg phosphatidylcholine, they showed that after binding of melittin to the *cis* side of the membrane, no charge could be detected on the *trans* side. This observation, however, does not exclude other models in which either the charge of the amino terminus is embedded in the bilayer, or the amino terminus is uncharged.

A wedge-like model, which is not excluded by our experiments, is that of Fig. 4C with $\theta_1 = \theta_2 = 20–30°$. The average orientation of the helical segments in this case is still predominantly perpendicular to the membrane plane with an angle between the two helical segments of 40–60°. In order to obtain this structure, the conformation of the bent region between amino acids 12–13 has to be changed considerably in comparison to that obtained from X-ray diffraction [11] and theoretical calculations [14].

Brown et al. [12] favor model C for the membrane-bound melittin because of NMR experiments performed with the peptide bound to detergent micelles. A structure was suggested from their results in which melittin penetrates only 6–8 Å into the hydrophobic interior of the micelle. In this context, it should be noted that Stoffel et al. [33] used 18-azidolinoleic acid as a photoreactive probe in phosphatidylcholine-melittin membranes, showing that melittin at least traverses half the lipid bilayer. A possible explanation for these diverse results may be a different orientation of melittin in a micelle and in a lipid bilayer, inspite of identical conformation, because of the small volume of the micelle and the curvature of its surface.

Finally, Kempf et al. [34] proposed a model similar to that of Fig. 4C. It was suggested that, under the influence of a transmembrane potential, the polypeptide goes reversibly from state C to state A. The model of this voltage-dependent transbilayer orientation of melittin was established in order to explain three experimental observations. (i) Addition of melittin to the *cis* side of a black lipid membrane induced an asymmetri voltage-dependent reversible conductance increase, when the potential was *trans*-negative. (ii) Addition of pronase to the *trans* side abolished the conductance only under the influence of a *trans*-negative potential. (iii) Trypsin abolished the conducting state of melittin only when added to the *cis* side. The model of a potential-induced movement of the N-terminus across the lipid bilayer is consonant with the experimental observations in Ref. 34. Nevertheless, we wish to point out that the experimental finding is a potential-dependent movement of the N-terminal segment toward the *trans* side of the membrane, making it accessible for pronase digestion. This does not necessarily imply that the N-terminus is located at the *cis* membrane side in the absence of an electric field. The experiments of Ref. 34 are also in agreement with model A, if a *trans* bilayer potential causes a small vertical displacement of the whole polypeptide and/or a change in the conformation of the bent region leading to a more stretched melittin molecule, thereby making the N-terminus accessible to enzymatic attack.

All our data are based on melittin in the ordered lipid bilayer at low water content. Further experiments have to be performed in order to show whether model A or C represents the actual orientation of melittin in a lipid membrane and, moreover, if full hydration or the physical state of the membrane may influence the orientation of the polypeptide.

References

1 Haberman, E. (1980) in Natural Toxins (Eaker, D. and Wadström, T., eds.), p. 173
2 Vogel, H. (1978) Dissertation, Universität Göttingen (1978)
3 Lavialle, F., Levin, I.W. and Mollay, C. (1980) Biochim. Biophys. Acta 600, 62
4 Vogel, H. (1981) Ber. Bunsenges. Phys. Chem. 85, 518
5 Jähnig, F., Vogel, H. and Best, L. (1982) Biochemistry 21, 6790
6 Segrest, J.P. and Feldmann, J.R. (1977) Biopolymers 16, 2053
7 Vogel, H. (1981) FEBS Lett. 134, 37
8 Lauterwein, J., Bösch, C., Brown, L.R. and Wüthrich, K. (1979) Biochim. Biophys. Acta 556, 244
9 Talbot, J.C., Dufourcq, J., De Bony, J., Faucon, J.F. and Lussan, C. (1979) FEBS Lett. 102, 191
10 Bello, J., Bello, R.H. and Granados, E. (1982) Biochemistry 21, 461
11 Terwilliger, L.C., Weissman, L. and Eisenberg, D. (1982) Biophys. J. 37, 353
12 Brown, L.R., Braun, W., Kumar, A. and Wüthrich, K. (1982) Biophys. J. 37, 319
13 Dawson, C.R., Drake, A.F., Helliwell, J. and Hider, R.C. (1978) Biochim. Biophys. Acta 510, 75
14 Pincus, M.R., Klausner, R.D. and Scheraga, H.A. (1982) Proc. Natl. Acad. Sci. U.S.A. 79, 5107
15 Brown, L.R. and Wüthrich, K. (1981) Biochim. Biophys. Acta 647, 95
16 Rothschild, K.J. and Clark, N.A. (1979) Biophys. J. 25, 473
17 Rothschild, K.J., Sanches, R., Hsiao, T.L. and Clark, N.A. (1980) Biophys. J. 31, 53
18 Nabedryk, E. and Breton, J. (1981) Biochim. Biophys. Acta 635, 515
19 Nabedryk, E., Gingold, M.P. and Breton, J. (1982) Biophys. J. 38, 243
20 Stümpel, J. (1982) Dissertation, Göttingen
21 Painter, P.C. and Koening, J.L. (1976) Biopolymers 15, 229
22 Fringelli, U.P. (1977) Z. Naturforsch. 32C, 20
23 Büldt, G., Gally, H.U., Seelig, J. and Zaccai, G. (1979) J. Mol. Biol. 134, 673
24 Janiak, M.J., Small, D.M. and Shipley, G.G. (1979) J. Biol. Chem. 254, 6068
25 Nevskaya, N.A. and Chirgadze, Y.N. (1976) Biopolymers 15, 637
26 Verma, S.P., Wallach, D.F.H. and Smith, I.C.P. (1974) Biochim. Biophys. Acta 345, 129
27 Peterson, N.O. and Chan, S.I. (1977) Biochem. 16, 2657
28 Vogel, H. and Jähnig, (1981) Chem. Phys. Lipids 29, 83
29 Oldfield, E., Kinsey, R.A. and Kintanar, A. (1982) Methods Enzymol. 88, 310
30 Engelman, D.M. and Steitz, T.A. (1981) Cell. 23, 411
31 Jähnig, F. (1983) Proc. Natl. Acad. Sci. U.S.A. 80, 3691
32 Schoch, P. and Sargent, D.F. (1980) Biochim. Biophys. Acta 602, 234
33 Stoffel, W., Schreiber, C. and Scheefers, H. (1978) Hoppe-Seyler's Z. Physiol. Chem. 259, 923
34 Kempf, C., Klausner, R.D., Weinstein, J.N., Van Renswoude, J., Pincus, M. and Blumenthal, R. (1982) J. Biol. Chem. 257, 2469